PHYSICAL REVIEW D **91,** 095024 (2015)

Search for a stable alignment limit in two-Higgs-doublet models

Dipankar Das[1,*] and Ipsita Saha[2,†]

[1]*Theory Physics Division, Saha Institute of Nuclear Physics, 1/AF Bidhan Nagar, Kolkata 700064, India*
[2]*Department of Theoretical Physics, Indian Association for the Cultivation of Science, 2A and 2B, Raja S.C. Mullick Road, Kolkata 700032, India*

(Received 16 April 2015; published 29 May 2015)

We study the conditions required to make the two-Higgs-doublet-model (2HDM) scalar potential stable up to the Planck scale. The lightest *CP*-even scalar is assumed to have been found at the LHC and the *alignment limit* is imposed in view of the LHC Higgs data. We find that ensuring stability up to scales $\gtrsim 10^{10}$ GeV necessitates the introduction of a soft breaking parameter in the theory. Even then, some interesting correlations between the nonstandard masses and the soft breaking parameter need to be satisfied. Consequently, a 2HDM becomes completely determined by only two nonstandard parameters, namely, $\tan\beta$ and a mass parameter, m_0, with $\tan\beta \gtrsim 3$. These observations make a 2HDM, in the *stable alignment limit*, more predictive than ever.

DOI: 10.1103/PhysRevD.91.095024 PACS numbers: 12.60.-i, 12.60.Fr, 14.80.Ec

I. INTRODUCTION

With the discovery of a Higgs-like particle at the Large Hadron Collider (LHC) [1,2], all the parameters of the Standard Model (SM) are now known and the fate of the SM is sealed. Taking all the uncertainties of the current experimental data into account, it has been found that the SM scalar potential becomes unstable somewhere within 10^8–10^{10} GeV [3–6]. In fact, it has been shown that for the SM scalar potential to be stable all the way up to the Planck scale ($M_P = 10^{19}$ GeV) the Higgs mass (m_h) needs to be in the following range [5]:

$$m_h > 129.6\ \text{GeV} + 2.0(M_t[\text{GeV}] - 173.34\ \text{GeV}) - 0.5\ \text{GeV}\left(\frac{\alpha_s(M_Z) - 0.1184}{0.0007}\right) \pm 0.3\ \text{GeV}, \qquad (1)$$

where M_t denotes the top quark pole mass and $\alpha_s(M_Z)$ is the strong coupling constant at the Z-boson mass scale. Hence, a SM Higgs boson with mass in the range 124–126 GeV certainly disfavors the possibility of having an absolutely stable vacuum up to M_P. As a way out of this vexing situation, it has been suggested that while absolute stability of the SM potential might be a tall ask, a metastable vacuum is entirely consistent with the current experimental value of the Higgs mass [4,7]. Nevertheless, the problem of vacuum stability in the SM remains one of the most discussed topics after the Higgs discovery and often has been taken as a hint for the intervention of some new physics.

Our objective in this paper is to investigate whether the two-Higgs-doublet models (2HDMs) [8] can do better in this respect. 2HDMs extend the scalar potential of the SM by adding one extra scalar doublet and therefore, rank amongst the simplest of beyond the Standard Model (BSM) constructions. For decades, 2HDMs have attracted a lot of attention because the minimal supersymmetry relies on a 2HDM scalar structure. Another attractive feature of 2HDMs is that the value of the electroweak ρ-parameter remains unity at the tree level. But one ominous consequence of introducing one additional scalar doublet is that now we will have two Yukawa matrices for each type of fermion and diagonalization of the fermion mass matrix will not guarantee the simultaneous diagonalization of the Yukawa matrices. As a result, there will be flavor changing neutral currents (FCNC), at the tree level, mediated by neutral scalars. This problem was addressed by Glashow and Weinberg [9] and independently by Paschos [10]. According to the Glashow-Weinberg-Paschos theorem, tree level FCNC can be avoided altogether if suitable arrangements are made such that fermions of a particular charge receive their masses from a particular scalar doublet. Usually, a Z_2 symmetry, under which $\phi_1 \to \phi_1$ and $\phi_2 \to -\phi_2$, is employed to achieve this. Proper assignments of the Z_2 charge to different fermions then complete the purpose. Labeling as ϕ_2 the doublet that couples to the up-type quarks, the following four conventional variants of 2HDMs emerge from the Z_2 charge assignments to the fermions:

(a) Type I: All quarks and leptons couple only to the doublet ϕ_2;
(b) Type II: ϕ_2 couples to the up-type quarks and ϕ_1 couples to down-type quarks and charged leptons;
(c) Type X or lepton specific: All quarks couple to ϕ_2, while ϕ_1 couples to the charged leptons;
(d) Type Y or flipped: Up-type quarks and charged leptons couple to ϕ_2 and all down-type quarks couple to ϕ_1.

*d.das@saha.ac.in
†tpis@iacs.res.in

Currently the measured values of Higgs signal strengths into different decay channels are consistent with the corresponding SM expectations. In anticipation that the data will continue to agree with the SM with increasing accuracy in the upcoming experiments, those BSM scenarios which can deliver a SM-like Higgs in some limiting case will hold the upper hand in the future survival race. It is quite well known that 2HDMs promise an *alignment limit* [11–13] when a SM-like Higgs can be recovered in the form of the lightest *CP*-even scalar in the 2HDM particle spectrum. Although vacuum stability constraints in 2HDMs have been studied previously both before [14] and after [15] the Higgs discovery, the distinct implications of the alignment limit in this context have never been emphasized before. Motivated by the LHC Higgs data, in this paper we concentrate exclusively on the alignment limit and explore the consequences of demanding the stability of the 2HDM potential all the way up to the grand unified theory (GUT) and Planck scales. In the process we have uncovered many new and interesting features. We have found that the requirement of stability of the 2HDM scalar potential compels us to introduce a soft breaking parameter and, at the same time, entails a strong correlation between the soft breaking parameter and the other nonstandard masses. Accordingly, in this "stable alignment limit" a 2HDM is completely determined by only two nonstandard parameters: (i) $\tan\beta(=v_2/v_1)$, which is the ratio of the two vacuum expectation values (vev's) and, (ii) a mass parameter (m_0). How the requirement of high scale stability of the 2HDM scalar potential in the alignment limit leads us to this intriguing conclusion constitutes the central theme of our paper.

The paper is organized in the following way: in Sec. II we describe the model and the various constraints that we use in our study. We present our results in Sec. III. In Sec. IV we summarize important findings and draw our conclusions.

II. THE SCALAR POTENTIAL

The general 2HDM potential with Z_2 symmetry under which $\phi_1 \to \phi_1$ and $\phi_2 \to -\phi_2$ is usually written as

$$\begin{aligned} V = {} & m_{11}^2\phi_1^\dagger\phi_1 + m_{22}^2\phi_2^\dagger\phi_2 - (m_{12}^2\phi_1^\dagger\phi_2 + \text{H.c.}) \\ & + \frac{\lambda_1}{2}(\phi_1^\dagger\phi_1)^2 + \frac{\lambda_2}{2}(\phi_2^\dagger\phi_2)^2 + \lambda_3(\phi_1^\dagger\phi_1)(\phi_2^\dagger\phi_2) \\ & + \lambda_4(\phi_1^\dagger\phi_2)(\phi_2^\dagger\phi_1) + \left\{\frac{\lambda_5}{2}(\phi_1^\dagger\phi_2)^2 + \text{H.c.}\right\}, \end{aligned} \tag{2}$$

where the term proportional to m_{12}^2 breaks the Z_2 symmetry softly. For simplicity, we assume that all the parameters of the potential are real so that *CP* symmetry is not explicitly broken in the scalar sector. To minimize the potential, we express the doublets as

$$\phi_i = \begin{pmatrix} \chi_i^+ \\ \frac{1}{\sqrt{2}}(h_i + i\eta_i) \end{pmatrix}, \tag{3}$$

and define the minimum as follows:

$$\langle\phi_i\rangle_{\min} = \begin{pmatrix} 0 \\ \frac{v_i}{\sqrt{2}} \end{pmatrix} \equiv \begin{pmatrix} 0 \\ \frac{(x_i+iy_i)}{\sqrt{2}} \end{pmatrix}. \tag{4}$$

Note that, although the potential of Eq. (2) is explicitly *CP* conserving, the vev's can, in general, be complex [16,17]. Now the minimization conditions will read as follows:

$$\begin{aligned} \left.\frac{\partial V}{\partial h_1}\right|_{\min} = {} & 2(m_{11}^2x_1 - m_{12}^2x_2) + \lambda_1x_1(x_1^2 + y_1^2) \\ & + x_1(\lambda_3 + \lambda_4)(x_2^2 + y_2^2) \\ & + \lambda_5(x_1x_2^2 + 2x_2y_1y_2 - x_1y_2^2) = 0, \end{aligned} \tag{5a}$$

$$\begin{aligned} \left.\frac{\partial V}{\partial h_2}\right|_{\min} = {} & 2(m_{22}^2x_2 - m_{12}^2x_1) + \lambda_2x_2(x_2^2 + y_2^2) \\ & + x_2(\lambda_3 + \lambda_4)(x_1^2 + y_1^2) \\ & + \lambda_5(x_2x_1^2 + 2x_1y_1y_2 - x_2y_1^2) = 0, \end{aligned} \tag{5b}$$

$$\begin{aligned} \left.\frac{\partial V}{\partial \eta_1}\right|_{\min} = {} & 2(m_{11}^2y_1 - m_{12}^2y_2) + \lambda_1y_1(x_1^2 + y_1^2) \\ & + y_1(\lambda_3 + \lambda_4)(x_2^2 + y_2^2) \\ & + \lambda_5(y_1y_2^2 + 2x_1x_2y_2 - x_2^2y_1) = 0, \end{aligned} \tag{5c}$$

$$\begin{aligned} \left.\frac{\partial V}{\partial \eta_2}\right|_{\min} = {} & 2(m_{22}^2y_2 - m_{12}^2y_1) + \lambda_2y_2(x_2^2 + y_2^2) \\ & + y_2(\lambda_3 + \lambda_4)(x_1^2 + y_1^2) \\ & + \lambda_5(y_2y_1^2 + 2x_1x_2y_1 - x_1^2y_2) = 0. \end{aligned} \tag{5d}$$

It can be easily checked that the choice $y_1 = y_2 = 0$, which implies the vev's are real, satisfies Eqs. (5c) and (5d) trivially. In this case, Eqs. (5a) and (5b) will take the following simpler forms:

$$\begin{aligned} \left.\frac{\partial V}{\partial h_1}\right|_{\min} = {} & 2(m_{11}^2v_1 - m_{12}^2v_2) \\ & + v_1\{\lambda_1v_1^2 + (\lambda_3 + \lambda_4 + \lambda_5)v_2^2\} = 0, \end{aligned} \tag{6a}$$

$$\begin{aligned} \left.\frac{\partial V}{\partial h_2}\right|_{\min} = {} & 2(m_{22}^2v_2 - m_{12}^2v_1) \\ & + v_2\{\lambda_2v_2^2 + (\lambda_3 + \lambda_4 + \lambda_5)v_1^2\} = 0. \end{aligned} \tag{6b}$$

Thus the assumption of real v_1 and v_2 is consistent with the minimization conditions of Eq. (5) and, in what follows, we shall work under this assumption.

When both the doublets receive vev's, the Z_2 symmetry is broken spontaneously too and we can rewrite the 2HDM potential in the following form [18]:

$$\begin{aligned} V = {} & \beta_1\left(\phi_1^\dagger\phi_1 - \frac{v_1^2}{2}\right)^2 + \beta_2\left(\phi_2^\dagger\phi_2 - \frac{v_2^2}{2}\right)^2 \\ & + \beta_3\left(\phi_1^\dagger\phi_1 + \phi_2^\dagger\phi_2 - \frac{v_1^2+v_2^2}{2}\right)^2 \\ & + \beta_4\{(\phi_1^\dagger\phi_1)(\phi_2^\dagger\phi_2) - (\phi_1^\dagger\phi_2)(\phi_2^\dagger\phi_1)\} \\ & + \beta_5\left(\mathrm{Re}\phi_1^\dagger\phi_2 - \frac{v_1 v_2}{2}\right)^2 + \beta_6(\mathrm{Im}\phi_1^\dagger\phi_2)^2. \end{aligned} \quad (7)$$

In comparison with the previous case, in this notation β_5 plays the role of the soft breaking parameter. For easy understanding of the future results, we will often switch between the parametrizations of Eqs. (2) and (7). Therefore, a comparison between the parameters of Eqs. (2) and (7) will be in order. It should be emphasized that unlike Eq. (2), Eq. (7) manifestly assumes that both the doublets acquire vev's so that m_{11}^2 and m_{22}^2 in Eq. (2) can be traded for v_1 and v_2 [using Eqs. (6a) and (6b)] followed by suitable rearrangements of the quartic parameters to obtain Eq. (7). Since, in this paper, we restrict ourselves only to the *noninert* cases where $\tan\beta$ is nonzero and finite, the above two parametrizations are equivalent to us. The connections between the two sets of parameters are given by the following relations:

$$\begin{aligned} & m_{11}^2 = -(\beta_1 v_1^2 + \beta_3 v^2); \qquad \lambda_1 = 2(\beta_1+\beta_3); \\ & m_{22}^2 = -(\beta_2 v_2^2 + \beta_3 v^2); \qquad \lambda_2 = 2(\beta_2+\beta_3); \\ & m_{12}^2 = \frac{\beta_5}{2} v_1 v_2; \qquad \lambda_3 = (2\beta_3+\beta_4); \\ & \lambda_4 = \frac{\beta_5+\beta_6}{2} - \beta_4; \qquad \lambda_5 = \frac{\beta_5-\beta_6}{2}. \end{aligned} \quad (8)$$

At this point, it is interesting to note that in the parametrization of Eq. (2), the combination $m_{12}^2/(\sin\beta\cos\beta)$ instead of m_{12}^2 itself controls the nonstandard masses [11]. Thus the relation between m_{12}^2 and β_5 in Eq. (8) suggests that β_5 is a better parameter for tracking the effect of soft breaking. In passing, we note that in the limit $\lambda_5 = 0$ [in Eq. (2)] or equivalently $\beta_5 = \beta_6$ [in Eq. (7)], the symmetry of the 2HDM potential is enhanced from softly broken Z_2 to softly broken $U(1)$, under which $\phi_1 \to \phi_1$ and $\phi_2 \to e^{i\theta}\phi_2$. This $U(1)$ symmetry will be relevant in our future discussions.

To get the mass eigenstates, we expand the scalar doublets around their vev's as follows:

$$\phi_i = \begin{pmatrix} \chi_i^+ \\ \frac{1}{\sqrt{2}}(v_i + h_i + i\eta_i) \end{pmatrix}. \quad (9)$$

Our assumption that CP is a good symmetry of the scalar potential actually allows us to define neutral scalar eigenstates that are also eigenstates of CP. In total, there are five physical eigenstates: two CP-even scalars (h, H), one CP-odd scalar (A) and a pair of charged scalars $(H^\pm)$ along with three Goldstones $(G^\pm, G^0)$ which will be absorbed to give masses to the SM gauge bosons $(W^\pm, Z)$. The rotations that lead us to the mass eigenstates are given below:

$$\begin{pmatrix} G^\pm \\ H^\pm \end{pmatrix} = \begin{pmatrix} c_\beta & s_\beta \\ -s_\beta & c_\beta \end{pmatrix}\begin{pmatrix} \chi_1^\pm \\ \chi_2^\pm \end{pmatrix}, \quad (10a)$$

$$\begin{pmatrix} G^0 \\ A \end{pmatrix} = \begin{pmatrix} c_\beta & s_\beta \\ -s_\beta & c_\beta \end{pmatrix}\begin{pmatrix} \eta_1 \\ \eta_2 \end{pmatrix}, \quad (10b)$$

$$\begin{pmatrix} h \\ H \end{pmatrix} = \begin{pmatrix} c_\alpha & s_\alpha \\ -s_\alpha & c_\alpha \end{pmatrix}\begin{pmatrix} h_1 \\ h_2 \end{pmatrix}, \quad (10c)$$

where $c_{\beta(\alpha)} \equiv \cos\beta(\alpha)$ and $s_{\beta(\alpha)} \equiv \sin\beta(\alpha)$. The mixing angle of the CP-even sector is defined through the following relation:

$$\tan 2\alpha = \frac{2(\beta_3 + \frac{\beta_5}{4})v_1 v_2}{\beta_1 v_1^2 - \beta_2 v_2^2 + (\beta_3 + \frac{\beta_5}{4})(v_1^2 - v_2^2)}. \quad (11)$$

It is now instructive to count the number of free parameters in the scalar potential. Note that Eqs. (2) and (7) both contain eight free parameters. In the notation of Eq. (7), these are v_1, v_2 and six β_i couplings. We can trade v_1 and v_2 for $v = \sqrt{v_1^2 + v_2^2}$ and $\tan\beta$. Except for β_5, all other β parameters may be traded for four physical scalar masses (m_h, m_H, m_A and m_{H^+}) and the angle, α. The equivalence of these two sets of parameters is demonstrated by the following relations:

$$\begin{aligned} \beta_1 = {} & \frac{1}{2v^2 c_\beta^2}\left[m_H^2 c_\alpha^2 + m_h^2 s_\alpha^2 - \frac{s_\alpha c_\alpha}{\tan\beta}(m_H^2 - m_h^2)\right] \\ & - \frac{\beta_5}{4}(\tan^2\beta - 1), \end{aligned} \quad (12a)$$

$$\begin{aligned} \beta_2 = {} & \frac{1}{2v^2 s_\beta^2}[m_h^2 c_\alpha^2 + m_H^2 s_\alpha^2 - s_\alpha c_\alpha \tan\beta(m_H^2 - m_h^2)] \\ & - \frac{\beta_5}{4}(\cot^2\beta - 1), \end{aligned} \quad (12b)$$

$$\beta_3 = \frac{1}{2v^2}\frac{s_\alpha c_\alpha}{s_\beta c_\beta}(m_H^2 - m_h^2) - \frac{\beta_5}{4}, \quad (12c)$$

$$\beta_4 = \frac{2}{v^2} m_{H^+}^2, \quad (12d)$$

$$\beta_6 = \frac{2}{v^2} m_A^2. \tag{12e}$$

Among the eight redefined parameters that appear on the rhs of Eq. (12), not all are unknown. We already know $v = 246$ GeV and, under the assumption that the lightest CP-even Higgs is what has been found at the LHC, $m_h \approx 125$ GeV is also known.

As a next level of simplification, we recall that the experimental values of the Higgs signal strengths into different decay modes are showing increasing affinity towards the SM expectations [19,20]. This encourages us to work in the alignment limit [11]:

$$\beta - \alpha = \frac{\pi}{2}, \tag{13}$$

which means h will have the exact SM-like tree level couplings with the fermions and the vector bosons. The recent global fits of the LHC data in the 2HDM context [21–27] certifies that Eq. (13) is indeed a reasonable assumption. In what follows, we will work exclusively in the alignment limit. Therefore, in this limit, we are left with five unknown parameters ($m_H, m_A, m_{H^+}, \beta_5$ and $\tan\beta$) which will be constrained from the requirement of high scale stability of the 2HDM potential. We will see that this requirement in association with the constraints from the electroweak T-parameter entail strong correlations between most of the remaining parameters, making the 2HDM more constrained than ever.

A. Theoretical constraints from vacuum stability and unitarity

First we have to ensure that there is not any direction in the field space along which the potential becomes infinitely negative. In the parametrization of Eq. (2), the necessary and sufficient conditions for the potential to be bounded from below read [28–31]

$$\text{VSC1}: \ \lambda_1 > 0, \tag{14a}$$

$$\text{VSC2}: \ \lambda_2 > 0, \tag{14b}$$

$$\text{VSC3}: \ \lambda_3 + \sqrt{\lambda_1 \lambda_2} > 0, \tag{14c}$$

$$\text{VSC4}: \ \lambda_3 + \lambda_4 - |\lambda_5| + \sqrt{\lambda_1 \lambda_2} > 0. \tag{14d}$$

The S-matrix eigenvalues that will be constrained from unitarity of the scattering amplitudes are also listed below [32–35]:

$$a_1^{\pm} = \frac{3}{2}(\lambda_1 + \lambda_2) \pm \sqrt{\frac{9}{4}(\lambda_1 - \lambda_2)^2 + (2\lambda_3 + \lambda_4)^2}, \tag{15a}$$

$$a_2^{\pm} = \frac{1}{2}(\lambda_1 + \lambda_2) \pm \frac{1}{2}\sqrt{(\lambda_1 - \lambda_2)^2 + 4\lambda_4^2}, \tag{15b}$$

$$a_3^{\pm} = \frac{1}{2}(\lambda_1 + \lambda_2) \pm \frac{1}{2}\sqrt{(\lambda_1 - \lambda_2)^2 + 4\lambda_5^2}, \tag{15c}$$

$$b_1^{\pm} = \lambda_3 + 2\lambda_4 \pm 3\lambda_5, \tag{15d}$$

$$b_2^{\pm} = \lambda_3 \pm \lambda_5, \tag{15e}$$

$$b_3^{\pm} = \lambda_3 \pm \lambda_4. \tag{15f}$$

The requirement of tree unitarity then restricts the above eigenvalues as follows:

$$|a_i^{\pm}|, |b_i^{\pm}| \leq 16\pi. \tag{16}$$

We impose that the inequalities (14) and (16) should be satisfied at all energies between the electroweak and Planck scales. The renormalization group (RG) equations that we use to calculate the lambdas at any intermediate energy scale are given in the Appendix.

Additionally it is also important to check whether the minimum defined by v_1 and v_2 is a global minimum or not. The condition for the global minimum, in the notation of Eq. (2), is given by [36,37]

$$\mathcal{D} = m_{12}^2 \left(m_{11}^2 - m_{22}^2 \sqrt{\frac{\lambda_1}{\lambda_2}} \right) \left(\tan\beta - \sqrt[4]{\frac{\lambda_1}{\lambda_2}} \right) > 0. \tag{17}$$

B. Experimental constraints

In addition to the theoretical constraints mentioned above, we also take the following experimental facts into account.

(a) There is a very strong lower limit on m_{H^+}, for type II models, arising mainly due to the excellent agreement of the $b \to s\gamma$ branching ratio with the SM prediction. Because of this we take $m_{H^+} > 300$ GeV [38,39] for type II models. However, if $\tan\beta > 1$, there is no such bound for type I models from flavor data [38]. Therefore, for type I models, we only consider the direct search limit $m_{H^+} > 80$ GeV [40]. At this stage, it should be noted that since the Yukawa couplings in the quark sector are the same for type II and Y models and the top Yukawa gives the dominant fermionic contribution in the RG equations, whatever we comment on type II models in this paper will eventually hold for type Y models too. The same is true for type I and X models.

(b) The oblique T-parameter can restrict the splitting between the heavy scalar masses. In the 2HDM alignment limit, the expression for the new physics contribution to the T-parameter can be expressed as [41,42]

$$\Delta T = \frac{1}{16\pi \sin^2\theta_w M_W^2}[F(m_{H^+}^2, m_H^2) + F(m_{H^+}^2, m_A^2) - F(m_H^2, m_A^2)], \quad (18)$$

$$\text{with} \quad F(x,y) = \begin{cases} \frac{x+y}{2} - \frac{xy}{x-y}\ln\left(\frac{x}{y}\right) & \text{for } x \neq y, \\ 0 & \text{for } x = y. \end{cases} \quad (19)$$

Taking the new physics contribution to the T-parameter as [43]

$$\Delta T = 0.05 \pm 0.12, \quad (20)$$

we use the 2σ uncertainty range around the mean value for our numerical constraints. Note that the function $F(x,y)$ is symmetric under $x \leftrightarrow y$ and is sensitive only to the difference $|x-y|$. Thus $\Delta T = 0$ when either $m_{H^+} = m_H$ or $m_{H^+} = m_A$. In these cases ΔT puts no constraints on the heavy scalar masses. But if, for some reason, $m_H \approx m_A$ then ΔT severely restricts the splitting between charged and neutral scalar masses.

III. NUMERICAL ANALYSIS AND RESULTS

For the purpose of analysis, we choose the set $\{v, \tan\beta, \alpha, m_h, m_H, m_A, m_{H^+}, \beta_5\}$ which appears on the rhs of Eq. (12) to be our independent set of eight parameters to describe the 2HDM scalar potential. Among them, we set $v = 246$ GeV and $\alpha = \beta - \pi/2$. In the case of an exact Z_2 symmetry we also set $\beta_5 = 0$ and perform a random scan for the rest of the parameters in the following ranges:

$$\begin{aligned} &\tan\beta \in [0.1, 10], \qquad m_h \in [124, 126]\ \text{GeV}, \\ &m_H \in [m_h, 1500]\ \text{GeV}, \qquad m_A \in [0, 1500]\ \text{GeV}, \\ &m_{H^+} \in [80, 1500]\ \text{GeV} \qquad \text{(for type I models)}, \\ &m_{H^+} \in [300, 1500]\ \text{GeV} \qquad \text{(for type II models)}. \end{aligned} \quad (21)$$

When the Z_2 symmetry is softly broken, we find it convenient to introduce the mass parameter

$$m_0 = \sqrt{\frac{1}{2}\beta_5 v^2}, \quad (22)$$

and vary m_0 in the range $[0, 1500]$ GeV. In the case of a softly broken $U(1)$ symmetry, we impose $m_0 = m_A$.

Next we use Eq. (12) to convert our set of parameters into the set of β_i's followed by Eq. (8) to convert the β_i's again into λ_i's. We then use the RG equations for λ_i's given in the Appendix to compute them at any intermediate energy scale and check that the unitarity and stability conditions hold all the way up to the Planck scale. We set the top quark pole mass at 173.3 GeV [44] for our numerical analysis. Our observations for different cases appear in the following subsections.

A. Exact Z_2

In this case setting $\beta_5 = 0$, we scan the rest of the parameters in the range specified previously. The result has been displayed in Fig. 1. A couple of noteworthy features that emerge from this figure are given below:

(i) The value of $\tan\beta$ is bounded and the bound depends on the energy scale, $\Lambda_{\rm UV}$, up to which stability is demanded. As we increase $\Lambda_{\rm UV}$, the allowed parameter space shrinks continuously. It should be noted that a limit on $\tan\beta$ for exact Z_2 symmetry is not surprising at all and is a direct consequence of unitarity and stability at the electroweak scale [45,46].

(ii) It is found that, for the noninert cases, neither type I nor type II models can be absolutely stable all the way up to the Planck scale when the Z_2 symmetry is exact in the potential. This result is in agreement with the previous analysis of Ref. [15] in the context of exact Z_2 symmetry. We have checked for each order of magnitude in $\Lambda_{\rm UV}$ and have noticed that type I models can remain stable up to a maximum of 10^8 GeV whereas type II models can be stable only up to 10^4 GeV. This difference between type I and type II models may be understood by noting that stability up to 10^8 GeV for type I models requires a light charged scalar, $m_{H^+} \sim 180$ GeV (see lower left panel of Fig. 1), which is not allowed for type II models from $b \to s\gamma$.

Now that we know 2HDMs with exact Z_2 symmetry fail to maintain stability up to the Planck scale, it is time to investigate whether the introduction of a soft symmetry breaking parameter can improve the situation.

B. Softly broken Z_2

Here we study the effects of nonzero β_5. For convenience we have encoded the information of β_5 into the mass parameter, m_0, through Eq. (22). The same analysis as in the case of exact Z_2 symmetry is then performed for three representative choices of $\Lambda_{\rm UV}$, namely, 10^{10}, 10^{16} and 10^{19} GeV. We exhibit our results in Figs. 2 and 3. Some intriguing features that emerge from these figures are listed below.

(a) From Figs. 2 and 3, we note that it is indeed possible for a 2HDM potential to remain stable all the way up to the Planck scale in the presence of a soft symmetry breaking parameter. But certain conditions need to be satisfied for this to happen. These conditions, which we describe below, together define the stable alignment limit for 2HDMs.

(b) From Fig. 2 we see that for the 2HDM potential to be stable up to $\Lambda_{\rm UV}$, there must exist a lower bound on

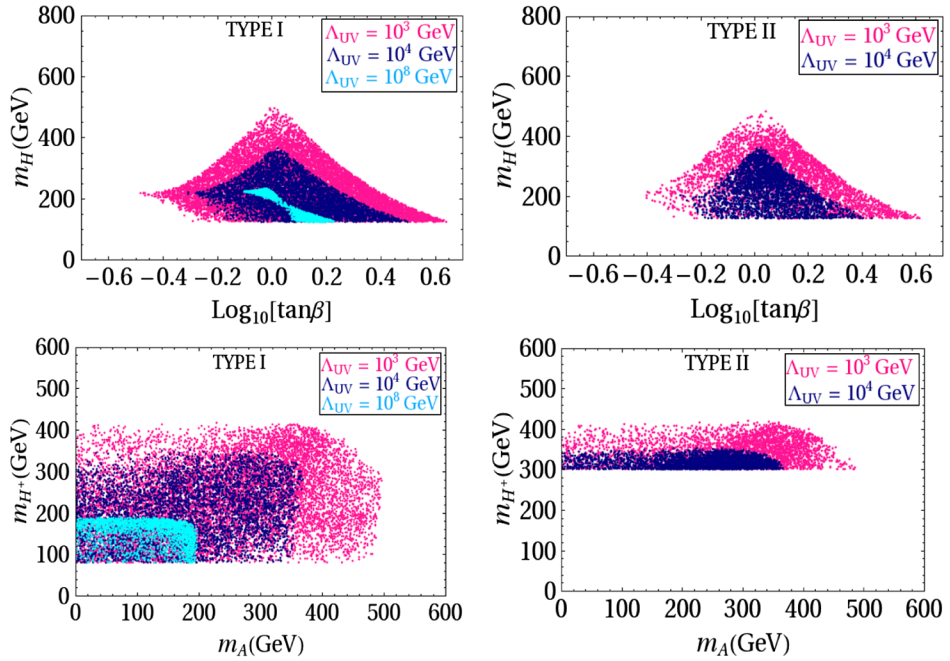

FIG. 1 (color online). Exact Z_2. Allowed points in the $\text{Log}_{10}(\tan\beta)$–$m_H$ and m_A-m_{H^+} planes for the 2HDM potential to be stable up to Λ_{UV}. The points in different colors correspond to different choices for Λ_{UV} which appear in the legends.

$\tan\beta$. For example, when $\Lambda_{UV} = 10^{19}$ GeV this bound reads $\tan\beta \gtrsim 3$. We also note from Fig. 2 that there is a lower limit on m_0 (or equivalently β_5) too. For type I models we read $m_0 \gtrsim 120$ GeV whereas for type II models we obtain $m_0 \gtrsim 280$ GeV. For the energy scales that we are concerned with, we observe that these limits on m_0 for type I and II models are essentially independent of Λ_{UV}. We emphasize that this is one of the important differences between our result and that of Ref. [15], where the stability of 2HDMs with softly broken Z_2 symmetry was analyzed including $\tan\beta = 2$ without realizing that such a low value of $\tan\beta$ is forbidden when the alignment limit is exact.

(c) From Fig. 3 we notice that the requirement of absolute stability up to Λ_{UV} entails a strong correlation between m_0 and the other nonstandard masses. In fact, a closer scrutiny of the plots reveals that all the nonstandard scalar masses have to be nearly degenerate with m_0.

(d) Observations (b) and (c) together lead us to the conclusion that, in the stable alignment limit, a 2HDM becomes completely determined by only two nonstandard parameters, namely, $\tan\beta$ and a mass parameter (m_0). Additionally, both of them are bounded from below:

$$\tan\beta \gtrsim 3, \qquad m_0 \gtrsim 120 \text{ GeV (type I)}, \quad m_0 \gtrsim 280 \text{ GeV (type II)}. \tag{23}$$

(e) We have also checked to see that the above conclusions do not crucially depend on the input parameters, especially the top quark mass. To be quantitative, instead of the central value of 173.3 GeV, if we consider the 2σ lower limit of the top quark pole

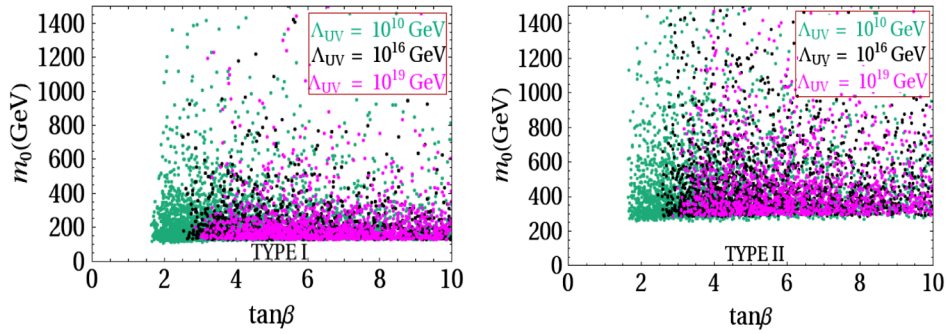

FIG. 2 (color online). Softly broken Z_2. Allowed points in $\tan\beta$–m_0 plane for the 2HDM potential to be stable up to Λ_{UV}. The points in different colors correspond to different choices for Λ_{UV} which appear in the legends.

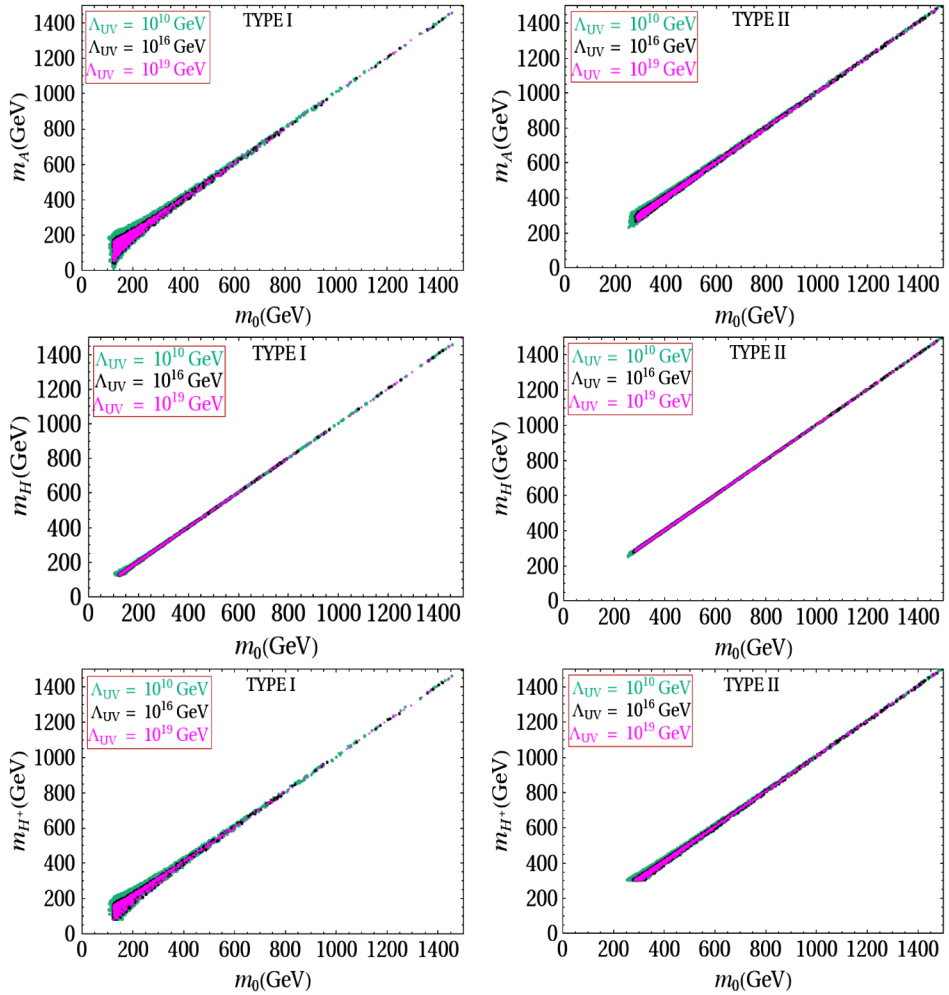

FIG. 3 (color online). Softly broken Z_2. Allowed points in the m_0-m_H, m_0-m_{H^+}, m_0-m_A planes for the 2HDM potential to be stable up to $\Lambda_{\rm UV}$. The points in different colors correspond to different choices for $\Lambda_{\rm UV}$ which appear in the legends.

mass, 171.8 GeV [44], the lower limit on $\tan\beta$ changes to $\tan\beta \gtrsim 2.8$.

We feel that an *a posteriori* explanation of most of the above features is possible, at least on a qualitative level. In the following we present, one by one, the steps of our argument that help us apprehend different characteristics of Figs. 2 and 3.

(1) First we note from Eq. (A7) in association with Eqs. (A8e), (A9e), (A10e) and (A11e) that the evolution of λ_5 is proportional to itself. This is not surprising because, as mentioned earlier, in the absence of λ_5 the symmetry of the scalar potential is enhanced to a global $U(1)$. Thus if we start with $\lambda_5 = 0$ at the electroweak scale, it will remain zero at all energy scales. But any initial nonzero value of λ_5 will cause it to grow with energy. This may eventually jeopardize the vacuum stability condition (14d) at high energy scales. Therefore, it will be no wonder if, by demanding high scale stability of the 2HDM potential, we are led to the $U(1)$ limit, $\lambda_5 \approx 0$. Evidently, this limit will have the following implication on the masses [using Eq. (12e) and remembering that $\lambda_5 \approx 0$ implies $\beta_5 \approx \beta_6$]:

$$m_A^2 \approx m_0^2, \tag{24}$$

which has been clearly depicted by the first row of plots in Fig. 3.

(2) The next important thing to note is that unitarity and stability conditions at the electroweak scale imply, among other things [46,47],

$$0 < (m_H^2 - m_0^2)(\tan^2\beta + \cot^2\beta) + 2m_h^2 < \frac{32\pi v^2}{3}. \tag{25}$$

This inequality has been plotted in Fig. 4 for three different values of $\tan\beta$. It is obvious that for $\tan\beta$ away from unity, the inequality (25) renders a degeneracy between m_H and m_0. This explains the second row of Fig. 3.

(3) Collecting (1) and (2) together we get $m_H^2 \approx m_A^2 \approx m_0^2$. Feeding this information to

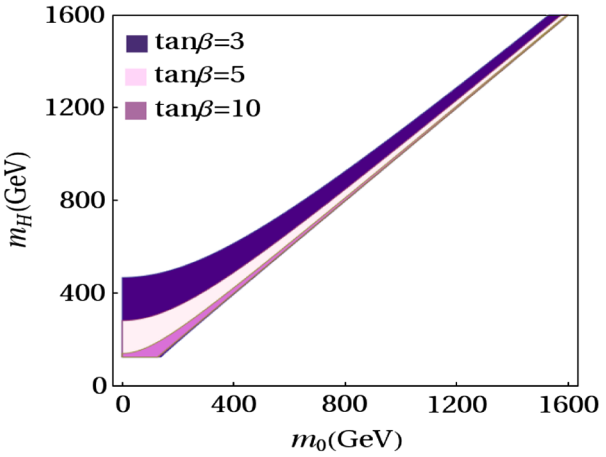

FIG. 4 (color online). Allowed regions in the m_0-m_H plane from the inequality (25) for three different values of $\tan\beta$.

Eq. (19), we obtain the following expression for ΔT:

$$\Delta T = \frac{1}{8\pi \sin^2\theta_w M_W^2} F(m_{H^+}^2, m_0^2). \quad (26)$$

Since $F(m_{H^+}^2, m_0^2)$ restricts the splitting $|m_{H^+}^2 - m_0^2|$, the experimental limit on ΔT will impart the degeneracy between m_{H^+} and m_0 as shown in Fig. 5. This explains the third row of Fig. 3.

Thus, up to this point, we have

$$m_0^2 \approx m_A^2 \approx m_H^2 \approx m_{H^+}^2, \quad (27)$$

which summarizes the essential features of Fig. 3 that the 2HDM can be described by a single nonstandard mass parameter. Equation (27) also explains the lower bounds on m_0 in Fig. 2. Since $m_{H^+} > 300$ GeV for type II 2HDMs, the degeneracy of Eq. (27) destroys the possibility of having a light

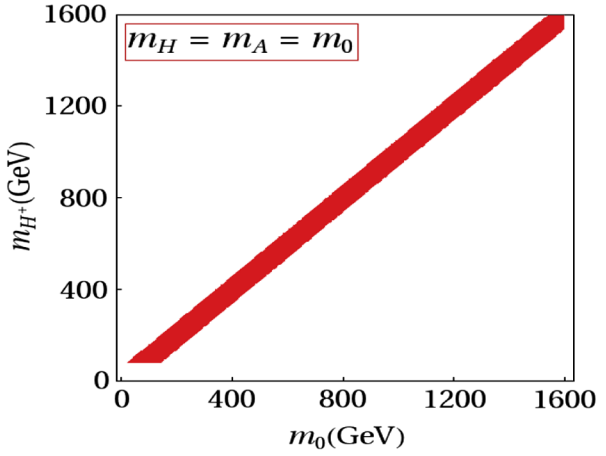

FIG. 5 (color online). Allowed region at 95% C.L. from the experimental limit on ΔT under the assumption $m_H = m_A = m_0$.

pseudoscalar for type II models. This result is apparent from the upper right panel of Fig. 3.

(4) To understand the lower limit on $\tan\beta$ we turn our attention to the RG evolution equation of λ_2 which is given by Eq. (A7) in association with Eqs. (A8b), (A9b), (A10b) and (A11b). Since we have assumed ϕ_2 to be the doublet that gives masses to the up-type quarks, λ_2 will face the negative pull of the top Yukawa (h_t). Note that in the limit of exact degeneracy, $m_0^2 = m_A^2 = m_H^2 = m_{H^+}^2$, we have at the electroweak scale [using Eq. (12) followed by Eq. (8) in the alignment limit],

$$\lambda_1 = \lambda_2 = \lambda_3 = \frac{m_h^2}{v^2}, \quad \text{and} \quad \lambda_4 = \lambda_5 = 0. \quad (28)$$

Using these, we may simplify the RG equation for λ_2, at the electroweak scale, as follows:

$$\begin{aligned}\mathcal{D}\lambda_2 = {} & 16\lambda_2^2 - 3(3g^2 + g'^2)\lambda_2 \\ & + \frac{3}{4}(3g^4 + g'^4 + 2g^2 g'^2) \\ & + 12h_t^2\lambda_2 - 12h_t^4. \end{aligned} \quad (29)$$

Notice the striking similarity between the above equation and the SM running of λ that appears in Eq. (A1). One difference is that $\mathcal{D}\lambda_2$ receives additional contributions on the positive side (compare $16\lambda_2^2$ with $12\lambda^2$ in the SM case) due to the presence of extra quartic couplings. On the contrary, h_t in the 2HDM case is $\sim\sqrt{2}m_t/(v\sin\beta)$, which is larger than the SM value of $h_t \sim \sqrt{2}m_t/v$. Therefore, compared to the SM case the negative drag of h_t is enhanced in 2HDMs. This effect drives λ_2 to negative values violating vacuum stability condition (14b) at high energies unless $\sin\beta$ is large enough to dilute the effect of the term, $-12h_t^4$, sufficiently. This is the origin of the lower limit on $\tan\beta$. Choosing $\tan\beta = 8.5$ for illustration, we have displayed this effect in Fig. 6. There we see how the evolution of the dotted (blue) line marked as VSC2 (which is nothing but λ_2) marginally survives becoming negative at an intermediate energy scale. Take $\tan\beta$ too low and this line goes below zero spoiling the stability condition, $\lambda_2 > 0$. It is worth noting that when all the nonstandard masses are exactly degenerate, evolutions of the λ_is depend only on $\tan\beta$ and not on the mass parameter, m_0.

(5) With exact degeneracy, the lower bound on $\tan\beta$ turns out to be $\tan\beta \gtrsim 8$ for $\Lambda_{\rm UV} = 10^{19}$ GeV. But from Fig. 2 we see that even lower values of $\tan\beta$ are allowed. To understand this, we need to investigate the evolution of λ_2 in greater detail. Instead of exact degeneracy, we now consider the following limit:

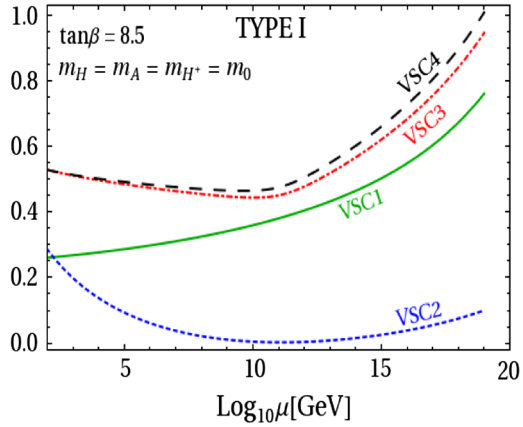

FIG. 6 (color online). Softly broken Z_2. Running of stability conditions of Eq. (14) in the exactly degenerate scenario assuming $m_h = 126$ GeV. In this scenario, these runnings are independent of m_0.

$$m_0 = m_A = m_H, \quad \text{and} \quad m_{H^+}^2 = m_0^2 + \Delta. \tag{30}$$

In this limit,

$$\lambda_1 = \lambda_2 = \frac{m_h^2}{v^2}, \qquad \lambda_3 = \lambda_2 + \frac{2\Delta}{v^2},$$
$$\lambda_4 = -\frac{2\Delta}{v^2}, \qquad \lambda_5 = 0. \tag{31}$$

Using these, we can rearrange the terms that appear on the rhs in the RG equation for λ_2 to obtain

$$\mathcal{D}\lambda_2 = 14\lambda_2^2 + 2\left(\lambda_2 + \frac{2\Delta}{v^2}\right)^2 - 3(3g^2 + g'^2)\lambda_2 + \frac{3}{4}(3g^4 + g'^4 + 2g^2g'^2) + 12h_t^2\lambda_2 - 12h_t^4. \tag{32}$$

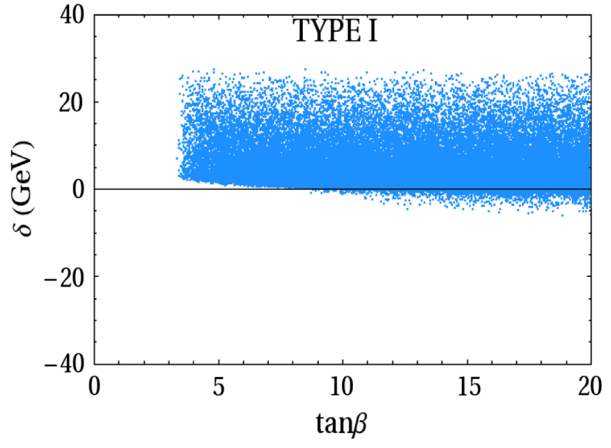

FIG. 7 (color online). Softly broken Z_2. Allowed points in the $\tan\beta$–δ plane for $\Lambda_{\rm UV} = 10^{19}$ GeV in a type I 2HDM with $m_H = m_A = m_0$, and $m_{H^+} = m_0 + \delta$.

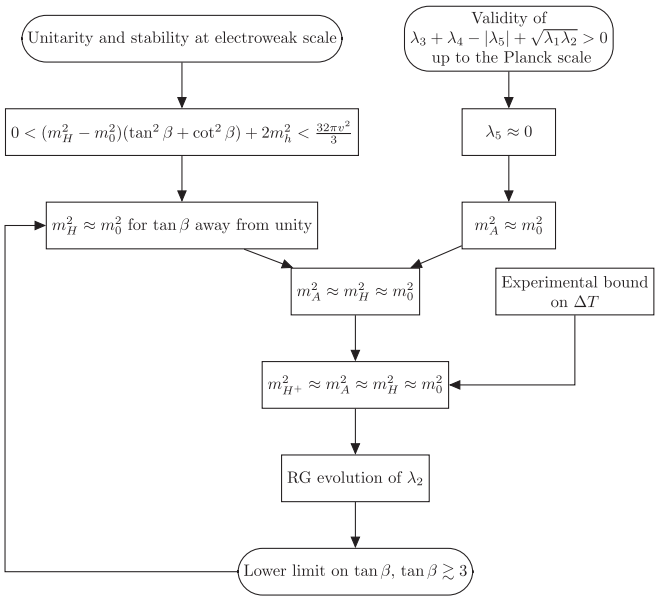

FIG. 8. Chain of arguments that helps us make sense of the main features of Figs. 2 and 3.

Comparing this with Eq. (29) we see that a positive value of Δ aids in the positive terms allowing lower values of $\tan\beta$. But the fact that only very small values of Δ can be permitted from unitarity [46] and the T-parameter puts a lower limit on $\tan\beta$ anyway. In Fig. 7 we have illustrated how the difference $\delta \equiv m_{H^+} - m_0 \approx \Delta/(2m_0)$ depends on $\tan\beta$. There we can see that to allow $\tan\beta \lesssim 8$ we will need $\delta > 0$, i.e., $m_{H^+} > m_0$.

We have summarized our arguments above compactly in the form of a flowchart in Fig. 8. Before moving on, we intend to make some remarks on the structure of the potential in the stable alignment limit. We note that in the limit, $m_0^2 = m_A^2 = m_H^2 = m_{H^+}^2$, the potential of Eq. (2) takes the following simple form[1]:

$$V = m_{11}^2\phi_1^\dagger\phi_1 + m_{22}^2\phi_2^\dagger\phi_2 - m_{12}^2(\phi_1^\dagger\phi_2 + \text{H.c.}) + \frac{\lambda_1}{2}(\phi_1^\dagger\phi_1 + \phi_2^\dagger\phi_2)^2. \tag{33}$$

This potential now contains four parameters among which two, disguised as v and m_h, have been measured. Two other parameters, in the form of $\tan\beta$ and m_0, remain to be determined to fix the model completely. Note that the symmetry in the quartic terms of Eq. (33) is more than a mere $U(1)$, in fact, the symmetry is enhanced to a global $U(2)$ under which $(\phi_1, \phi_2)^T \to U(2)(\phi_1, \phi_2)^T$. But this $U(2)$ symmetry is explicitly broken in the Yukawa terms. Due to this, the structure of the potential in Eq. (33) is not

[1]Similar potential can also be motivated from an $SO(5)$ symmetry [48].

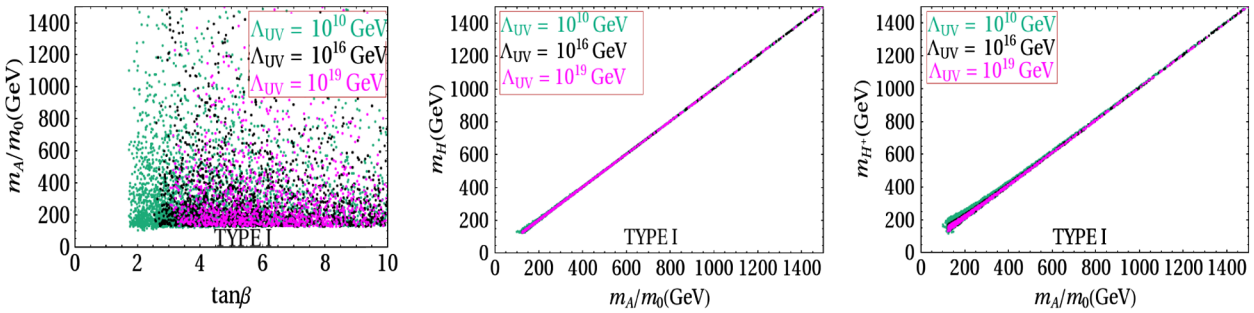

FIG. 9 (color online). Softly broken $U(1)$. Allowed points in the $\tan\beta$–m_A, m_A-m_H, m_A-m_{H^+} planes for the 2HDM potential to be stable up to $\Lambda_{\rm UV}$. Three different colors correspond to three different choices of $\Lambda_{\rm UV}$ which appear in the legends.

stable under RG. Neither the correlation $\lambda_1 = \lambda_2 = \lambda_3$ nor the equality $\lambda_4 = 0$ is maintained at higher energies. What remains valid at any scale is the equality $\lambda_5 = 0$ because the $U(1)$ symmetry that prevails in the quartic part of the scalar potential in the absence of λ_5 is also preserved in the Yukawa sector by construction. Therefore, we conclude that when high scale stability of the 2HDM potential needs to be ensured, softly broken $U(1)$ symmetry should be a more natural choice, to tackle tree level FCNC, than the conventional Z_2 symmetry.

Now we want to check to see whether the condition (17) for the global minimum holds in the stable alignment limit or not. First we remember that, in this limit, m_0 is positive (see Fig. 2) which implies $m_{12}^2 > 0$. We have also found $\lambda_1 \approx \lambda_2 \approx \lambda_3$ with $\tan\beta \gtrsim 3$. These imply

$$\left(\tan\beta - \sqrt[4]{\frac{\lambda_1}{\lambda_2}}\right) > 0. \tag{34a}$$

The remaining factor in Eq. (17) can be evaluated, in the stable alignment limit, as follows:

$$m_{11}^2 - m_{22}^2\sqrt{\frac{\lambda_1}{\lambda_2}} \approx m_{11}^2 - m_{22}^2$$

$$= \beta_2 v_2^2 - \beta_1 v_1^2 \quad [\text{using Eq. (8)}], \tag{34b}$$

$$= m_A^2(\sin^2\beta - \cos^2\beta) \quad [\text{using Eq. (12) with } m_0 \approx m_A], \tag{34c}$$

$$= m_A^2\cos^2\beta(\tan^2\beta - 1) > 0 \quad [\because \tan\beta \gtrsim 3]. \tag{34d}$$

Therefore we conclude that, in the stable alignment limit, condition (17) is satisfied automatically and hence, existence of the global minimum is guaranteed.

C. Softly broken $U(1)$

Here we will have $m_A = m_0$ from the beginning. Evidently, when the $U(1)$ symmetry is exact in the potential, i.e., $m_0 = 0$, A will become the Goldstone boson. We present the result of our analysis, for type I models, in Fig. 9. Although these plots do not provide any new insights, we include them just for completeness. The interpretation of Fig. 9 will be similar to that of the corresponding plots in the case of softly broken Z_2 symmetry.

IV. SUMMARY AND CONCLUSIONS

In this paper we have studied the consequences of demanding absolute stability of the 2HDM potential all the way up to the Planck scale. In view of the fact that the LHC Higgs data are in conformity with the SM expectations, we decided to work in the alignment limit where the lightest CP-even scalar (h) possesses SM-like tree level couplings with the *standard* particles. Although we have explicitly demonstrated our results for type I and II models only, they are equally applicable to type X and Y models also. We have found that, in the alignment limit, requirement of high scale stability puts some remarkable restrictions on the 2HDM parameter space. This set of restrictions defines the stable alignment limit for 2HDMs. Some of our most important observations are summarized below:

(a) The 2HDM scalar potential with an exact Z_2 symmetry is unable to maintain stability after 10^8 GeV (10^4 GeV) in the type I (II) case. To ensure stability up to the Planck scale, Z_2 symmetry needs to be broken softly.
(b) By demanding high scale stability in the presence of a soft breaking, we are led to a situation where the symmetry of the potential is enhanced from softly broken Z_2 to softly broken $U(1)$.
(c) To have stability up to very high energies ($\gtrsim 10^{10}$ GeV), all the nonstandard masses need to be nearly degenerate: $m_0 \approx m_A \approx m_H \approx m_{H^+}$. Thus, there is only one nonstandard mass parameter that governs the 2HDM in the stable alignment limit.
(d) The value of $\tan\beta$ is bounded from below.

Therefore, in the stable alignment limit, a 2HDM can be fully described by only two new parameters, namely, $\tan\beta$ and m_0 with $\tan\beta \gtrsim 3$ and $m_0 \gtrsim 120$ GeV (280 GeV) for type I (II) models.

Finally, we end the paper on a pessimistic note. One should remember that, in the alignment limit, even the

self-couplings of h are identical to the SM at tree level. This means, in this limit, any measurement involving the standard particles can smell the presence of nonstandard physics only through loop effects. But then the nonstandard particles can be made heavy enough to dilute these effects sufficiently. Thus, our only hope to detect the presence of nonstandard scalars beyond the reaches of the direct search experiments is via some nondecoupling effects in certain loop induced processes like Higgs to diphoton decay [49]. But with the degeneracy, $m_0^2 \approx m_{H^+}^2$, this possibility is also eliminated. Therefore, it appears that even if the LHC data continues to agree with the SM predictions, a 2HDM in the stable alignment limit which is very difficult, if not impossible, to probe experimentally, can serve as an alternative to the SM for many years to come.

ACKNOWLEDGMENTS

D. D. thanks the Department of Atomic Energy (DAE), India for their financial support.

APPENDIX: ONE LOOP RG EQUATIONS

Let us first write down the one loop RG equation (RGE) of the SM quartic coupling (λ) [50,51] as follows:

$$\mathcal{D}\lambda = 12\lambda^2 - 3(3g^2 + g'^2)\lambda + \frac{3}{4}(3g^4 + g'^4 + 2g^2g'^2) + 12h_t^2\lambda - 12h_t^4, \tag{A1}$$

where h_t denotes the top Yukawa which dominates over the other Yukawa couplings. For convenience, we have introduced the shorthand $\mathcal{D} \equiv 16\pi^2 \frac{\mathrm{d}}{\mathrm{d}(\ln\mu)}$.

Now we will present the one loop RGEs of all the relevant couplings (gauge, Yukawa and scalar quartic couplings) of the 2HDM [8,52–54].

1. Gauge couplings

RGEs for the gauge couplings,

$$\mathcal{D}g_s = -7g_s^3, \tag{A2a}$$

$$\mathcal{D}g = -3g^3, \tag{A2b}$$

$$\mathcal{D}g' = 7g'^3. \tag{A2c}$$

2. Yukawa couplings

The initial values of top (h_t), bottom (h_b) and tau (h_τ) Yukawa couplings at electroweak scale (M_t) for the different Yukawa structures are given by

$$\text{type I:} \begin{cases} h_t(M_t) &= \frac{\sqrt{2}M_t}{v\sin\beta}\{1 - \frac{4}{3\pi}\alpha_s(M_t)\}, \\ h_{b,\tau}(M_t) &= \frac{\sqrt{2}m_{b,\tau}}{v\sin\beta}; \end{cases} \tag{A3a}$$

$$\text{type II:} \begin{cases} h_t(M_t) &= \frac{\sqrt{2}M_t}{v\sin\beta}\{1 - \frac{4}{3\pi}\alpha_s(M_t)\}, \\ h_{b,\tau}(M_t) &= \frac{\sqrt{2}m_{b,\tau}}{v\cos\beta}; \end{cases} \tag{A3b}$$

where $\alpha_s(M_t)$ denotes the strong coupling constant at top quark pole mass. The corresponding RGEs for the type I Yukawa structure are given by

$$\mathcal{D}h_t = h_t\left(a_u + \frac{9}{2}h_t^2 + \frac{3}{2}h_b^2 + h_\tau^2\right), \tag{A4a}$$

$$\mathcal{D}h_b = h_b\left(a_d + \frac{3}{2}h_t^2 + \frac{9}{2}h_b^2 + h_\tau^2\right), \tag{A4b}$$

$$\mathcal{D}h_\tau = h_\tau\left(a_e + 3h_t^2 + 3h_b^2 + \frac{5}{2}h_\tau^2\right). \tag{A4c}$$

For the type II Yukawa structure, the RGEs take the following form:

$$\mathcal{D}h_t = h_t\left(a_u + \frac{9}{2}h_t^2 + \frac{1}{2}h_b^2\right), \tag{A5a}$$

$$\mathcal{D}h_b = h_b\left(a_d + \frac{1}{2}h_t^2 + \frac{9}{2}h_b^2 + h_\tau^2\right), \tag{A5b}$$

$$\mathcal{D}h_\tau = h_\tau\left(a_e + 3h_b^2 + \frac{5}{2}h_\tau^2\right), \tag{A5c}$$

where

$$a_u = \left(-8g_s^2 - \frac{9}{4}g^2 - \frac{17}{12}g'^2\right), \tag{A6a}$$

$$a_d = \left(-8g_s^2 - \frac{9}{4}g^2 - \frac{5}{12}g'^2\right), \tag{A6b}$$

$$a_e = \left(-\frac{9}{4}g^2 - \frac{15}{4}g'^2\right), \tag{A6c}$$

for both type I and II models.

3. Scalar quartic couplings

The RGEs for the five quartic couplings that appear in Eq. (2) are given by

$$\mathcal{D}\lambda_i = \beta_{\lambda_i} + G_i + H_i, \qquad (i = 1, 2, 3, 4, 5), \tag{A7}$$

where β_{λ_i} and G_i are independent of the Yukawa structure of the model and are as follows:

$$\beta_{\lambda_1} = 12\lambda_1^2 + 4\lambda_3^2 + 4\lambda_3\lambda_4 + 2\lambda_4^2 + 2\lambda_5^2, \tag{A8a}$$

$$\beta_{\lambda_2} = 12\lambda_2^2 + 4\lambda_3^2 + 4\lambda_3\lambda_4 + 2\lambda_4^2 + 2\lambda_5^2, \quad \text{(A8b)}$$

$$\beta_{\lambda_3} = (\lambda_1 + \lambda_2)(6\lambda_3 + 2\lambda_4) + 4\lambda_3^2 + 2\lambda_4^2 + 2\lambda_5^2, \quad \text{(A8c)}$$

$$\beta_{\lambda_4} = 2\lambda_4(\lambda_1 + \lambda_2) + 8\lambda_3\lambda_4 + 4\lambda_4^2 + 8\lambda_5^2, \quad \text{(A8d)}$$

$$\beta_{\lambda_5} = \lambda_5(2\lambda_1 + 2\lambda_2 + 8\lambda_3 + 12\lambda_4), \quad \text{(A8e)}$$

and

$$G_1 = \frac{3}{4}(3g^4 + g'^4 + 2g^2g'^2) - 3\lambda_1(3g^2 + g'^2), \quad \text{(A9a)}$$

$$G_2 = \frac{3}{4}(3g^4 + g'^4 + 2g^2g'^2) - 3\lambda_2(3g^2 + g'^2), \quad \text{(A9b)}$$

$$G_3 = \frac{3}{4}(3g^4 + g'^4 - 2g^2g'^2) - 3\lambda_3(3g^2 + g'^2), \quad \text{(A9c)}$$

$$G_4 = 3g^2g'^2 - 3\lambda_4(3g^2 + g'^2), \quad \text{(A9d)}$$

$$G_5 = -3\lambda_5(3g^2 + g'^2). \quad \text{(A9e)}$$

The expressions for the H_i's, however, depend on the Yukawa structure of the model. For type I models, these are given by

$$H_1 = 0, \quad \text{(A10a)}$$

$$H_2 = 4\lambda_2(3h_t^2 + 3h_b^2 + h_\tau^2) - (12h_t^4 + 12h_b^4 + 4h_\tau^4), \quad \text{(A10b)}$$

$$H_3 = 2\lambda_3(3h_t^2 + 3h_b^2 + h_\tau^2), \quad \text{(A10c)}$$

$$H_4 = 2\lambda_4(3h_t^2 + 3h_b^2 + h_\tau^2), \quad \text{(A10d)}$$

$$H_5 = 2\lambda_5(3h_t^2 + 3h_b^2 + h_\tau^2). \quad \text{(A10e)}$$

For the type II Yukawa structure, we have

$$H_1 = 4\lambda_1(3h_b^2 + h_\tau^2) - (12h_b^4 + 4h_\tau^4), \quad \text{(A11a)}$$

$$H_2 = 12\lambda_2h_t^2 - 12h_t^4, \quad \text{(A11b)}$$

$$H_3 = 2\lambda_3(3h_t^2 + 3h_b^2 + h_\tau^2) - 12h_t^2h_b^2, \quad \text{(A11c)}$$

$$H_4 = 2\lambda_4(3h_t^2 + 3h_b^2 + h_\tau^2) + 12h_t^2h_b^2, \quad \text{(A11d)}$$

$$H_5 = 2\lambda_5(3h_t^2 + 3h_b^2 + h_\tau^2). \quad \text{(A11e)}$$

[1] G. Aad *et al.* (ATLAS Collaboration), Observation of a new particle in the search for the Standard Model Higgs boson with the ATLAS detector at the LHC, Phys. Lett. B **716**, 1 (2012).

[2] S. Chatrchyan *et al.* (CMS Collaboration), Observation of a new boson at a mass of 125 GeV with the CMS experiment at the LHC, Phys. Lett. B **716**, 30 (2012).

[3] F. Bezrukov, M. Y. Kalmykov, B. A. Kniehl, and M. Shaposhnikov, Higgs boson mass and new physics, J. High Energy Phys. 10 (2012) 140.

[4] G. Degrassi, S. Di Vita, J. Elias-Miro, J. R. Espinosa, G. F. Giudice, G. Isidori, and A. Strumia, Higgs mass and vacuum stability in the Standard Model at NNLO, J. High Energy Phys. 08 (2012) 098.

[5] D. Buttazzo, G. Degrassi, P. P. Giardino, G. F. Giudice, F. Sala, A. Salvio, and A. Strumia, Investigating the near-criticality of the Higgs boson, J. High Energy Phys. 12 (2013) 089.

[6] V. Branchina and E. Messina, Stability, Higgs Boson Mass, and New Physics, Phys. Rev. Lett. **111**, 241801 (2013).

[7] V. Branchina, E. Messina, and M. Sher, Lifetime of the electroweak vacuum and sensitivity to Planck scale physics, Phys. Rev. D **91**, 013003 (2015).

[8] G. Branco, P. Ferreira, L. Lavoura, M. Rebelo, M. Sher, and J. P. Silva, Theory and phenomenology of two-Higgs-doublet models, Phys. Rep. **516**, 1 (2012).

[9] S. L. Glashow and S. Weinberg, Natural conservation laws for neutral currents, Phys. Rev. D **15**, 1958 (1977).

[10] E. Paschos, Diagonal neutral currents, Phys. Rev. D **15**, 1966 (1977).

[11] J. F. Gunion and H. E. Haber, The *CP* conserving two Higgs doublet model: The approach to the decoupling limit, Phys. Rev. D **67**, 075019 (2003).

[12] N. Craig and S. Thomas, Exclusive signals of an extended Higgs sector, J. High Energy Phys. 11 (2012) 083.

[13] M. Carena, I. Low, N. R. Shah, and C. E. Wagner, Impersonating the Standard Model Higgs boson: Alignment without decoupling, J. High Energy Phys. 04 (2014) 015.

[14] P. Ferreira and D. Jones, Bounds on scalar masses in two Higgs doublet models, J. High Energy Phys. 08 (2009) 069.

[15] N. Chakrabarty, U. K. Dey, and B. Mukhopadhyaya, High-scale validity of a two-Higgs doublet scenario: A study including LHC data, J. High Energy Phys. 12 (2014) 166.

[16] J. F. Gunion and H. E. Haber, Conditions for *CP* violation in the general two-Higgs-doublet model, Phys. Rev. D **72**, 095002 (2005).

[17] P. Ferreira, M. Maniatis, O. Nachtmann, and J. P. Silva, *CP* properties of symmetry-constrained two-Higgs-doublet models, J. High Energy Phys. 08 (2010) 125.

[18] J. F. Gunion, H. E. Haber, G. L. Kane, and S. Dawson, The Higgs hunter's guide, Front. Phys. **80**, 1 (2000).

[19] ATLAS Collaboration, Report No. ATLAS-CONF-2014-009, 2014.
[20] CMS Collaboration, Precise determination of the mass of the Higgs boson and studies of the compatibility of its couplings with the standard model.
[21] B. Coleppa, F. Kling, and S. Su, Constraining type II 2HDM in light of LHC Higgs searches, J. High Energy Phys. 01 (2014) 161.
[22] C.-Y. Chen, S. Dawson, and M. Sher, Heavy higgs searches and constraints on two Higgs doublet models, Phys. Rev. D **88**, 015018 (2013); **88**, 039901 (2013).
[23] N. Craig, J. Galloway, and S. Thomas, Searching for signs of the second Higgs doublet, arXiv:1305.2424.
[24] O. Eberhardt, U. Nierste, and M. Wiebusch, Status of the two-Higgs-doublet model of type II, J. High Energy Phys. 07 (2013) 118.
[25] B. Dumont, J. F. Gunion, Y. Jiang, and S. Kraml, Constraints on and future prospects for two-Higgs-doublet models in light of the LHC Higgs signal, Phys. Rev. D **90**, 035021 (2014).
[26] B. Dumont, J. F. Gunion, Y. Jiang, and S. Kraml, Addendum to "Constraints on and future prospects for two-Higgs-doublet models in light of the LHC Higgs signal," arXiv:1409.4088.
[27] J. Bernon, B. Dumont, and S. Kraml, Status of Higgs couplings after run 1 of the LHC, Phys. Rev. D **90**, 071301 (2014).
[28] N. G. Deshpande and E. Ma, Pattern of symmetry breaking with two Higgs doublets, Phys. Rev. D **18**, 2574 (1978).
[29] K. Klimenko, On necessary and sufficient conditions for some Higgs potentials to be bounded from below, Theor. Math. Phys. **62**, 58 (1985).
[30] B. M. Kastening, Bounds from stability and symmetry breaking on parameters in the two Higgs doublet potential, arXiv:hep-ph/9307224.
[31] M. Maniatis, A. von Manteuffel, O. Nachtmann, and F. Nagel, Stability and symmetry breaking in the general two-Higgs-doublet model, Eur. Phys. J. C **48**, 805 (2006).
[32] J. Maalampi, J. Sirkka, and I. Vilja, Tree level unitarity and triviality bounds for two Higgs models, Phys. Lett. B **265**, 371 (1991).
[33] S. Kanemura, T. Kubota, and E. Takasugi, Lee-Quigg-Thacker bounds for Higgs boson masses in a two doublet model, Phys. Lett. B **313**, 155 (1993).
[34] A. G. Akeroyd, A. Arhrib, and E.-M. Naimi, Note on tree level unitarity in the general two Higgs doublet model, Phys. Lett. B **490**, 119 (2000).
[35] J. Horejsi and M. Kladiva, Tree-unitarity bounds for THDM Higgs masses revisited, Eur. Phys. J. C **46**, 81 (2006).
[36] A. Barroso, P. Ferreira, I. Ivanov, R. Santos, and J. P. Silva, Evading death by vacuum, Eur. Phys. J. C **73**, 2537 (2013).
[37] A. Barroso, P. Ferreira, I. Ivanov, and R. Santos, Metastability bounds on the two Higgs doublet model, J. High Energy Phys. 06 (2013) 045.
[38] F. Mahmoudi and O. Stal, Flavor constraints on the two-Higgs-doublet model with general Yukawa couplings, Phys. Rev. D **81**, 035016 (2010).
[39] O. Deschamps, S. Descotes-Genon, S. Monteil, V. Niess, S. T'Jampens, and V. Tisserand, Two Higgs doublet of type II facing flavor physics data, Phys. Rev. D **82**, 073012 (2010).
[40] LEP Higgs Working Group and ALEPH, DELPHI, L3, and OPAL Collaborations, Search for charged Higgs bosons: Preliminary combined results using LEP data collected at energies up to 209 GeV, arXiv:hep-ex/0107031.
[41] H.-J. He, N. Polonsky, and S.-f. Su, Extra families, Higgs spectrum, and oblique corrections, Phys. Rev. D **64**, 053004 (2001).
[42] W. Grimus, L. Lavoura, O. Ogreid, and P. Osland, A precision constraint on multi-Higgs-doublet models, J. Phys. G **35**, 075001 (2008).
[43] M. Baak and R. Kogler, The global electroweak Standard Model fit after the Higgs discovery, arXiv:1306.0571.
[44] ATLAS, CDF, CMS, and D0 Collaborations, First combination of Tevatron and LHC measurements of the top-quark mass, arXiv:1403.4427.
[45] B. Swiezewska, Yukawa independent constraints for two-Higgs-doublet models with a 125 GeV Higgs boson, Phys. Rev. D **88**, 055027 (2013); **88**, 119903(E) (2013).
[46] D. Das, New limits on $\tan\beta$ for 2HDMs with Z_2 symmetry, arXiv:1501.02610.
[47] G. Bhattacharyya, D. Das, P. B. Pal, and M. Rebelo, Scalar sector properties of two-Higgs-doublet models with a global $U(1)$ symmetry, J. High Energy Phys. 10 (2013) 081.
[48] P. B. Dev and A. Pilaftsis, Maximally symmetric two Higgs doublet model with natural standard model alignment, J. High Energy Phys. 12 (2014) 024.
[49] G. Bhattacharyya and D. Das, Nondecoupling of charged scalars in Higgs decay to two photons and symmetries of the scalar potential, Phys. Rev. D **91**, 015005 (2015).
[50] H. Arason, D. Castano, B. Keszthelyi, S. Mikaelian, E. J. Piard, P. Ramond, and B. D. Wright, Renormalization-group study of the standard model and its extensions: The standard model, Phys. Rev. D **46**, 3945 (1992).
[51] M.-x. Luo and Y. Xiao, Two-Loop Renormalization Group Equations in the Standard Model, Phys. Rev. Lett. **90**, 011601 (2003).
[52] H. E. Haber and R. Hempfling, Renormalization-group-improved Higgs sector of the minimal supersymmetric model, Phys. Rev. D **48**, 4280 (1993).
[53] W. Grimus and L. Lavoura, Renormalization of the neutrino mass operators in the multi-Higgs-doublet standard model, Eur. Phys. J. C **39**, 219 (2005).
[54] P. Ferreira, L. Lavoura, and J. P. Silva, Renormalization-group constraints on Yukawa alignment in multi-Higgs-doublet models, Phys. Lett. B **688**, 341 (2010).